

The Serotonin Binding Site of Human and Murine 5-HT_{2B} Receptors

MOLECULAR MODELING AND SITE-DIRECTED MUTAGENESIS*

Received for publication, January 8, 2002

Published, JBC Papers in Press, February 21, 2002, DOI 10.1074/jbc.M200195200

Philippe Manivet^{‡§}, Benoît Schneider[¶], Jeremy Christopher Smith^{||}, Doo-Sup Choi^{**},
Luc Maroteaux^{**}, Odile Kellermann[¶], and Jean-Marie Launay^{‡ ‡‡}

From the [‡]Centre de Recherche Claude Bernard Pathologie Expérimentale et Communications Cellulaires, IFR 6, Service de Biochimie, Hôpital Lariboisière Assistance Publique-Hopitaux de Paris (AP-HP), 75475 Paris Cedex 10, France, [§]Laboratoire Département de Chimie des Mécanismes Réactionnels (DCMR), Ecole Polytechnique, 91112 Palaiseau, France, [¶]Différenciation Cellulaire, UPR 1983 CNRS, Institut André Lwoff, 94801 Villejuif, France, ^{||}Leturstuhl für Biocomputing, IWR der Universität Heidelberg, D-69120 Heidelberg, Germany, and ^{**}Institut de Génétique et de Biologie Moléculaire et Cellulaire, CNRS/INSERM, Université de Strasbourg, BP 163 67404 Illkirch, France

Bacteriorhodopsin and rhodopsin crystal structures were used as templates to build structural models of the mouse and human serotonin (5-HT)-2B receptors (5-HT_{2B}Rs). Serotonin was docked to the receptors, and the amino acids predicted to participate to its binding were subjected to mutagenesis. 5-HT binding affinity and 5-HT-induced inositol triphosphate production were measured in LMTK⁻ cells transfected with either wild-type or mutated receptor genes. According to these measurements, the bacteriorhodopsin-based models of the 5-HT_{2B}Rs appear more confident than the rhodopsin-based ones. Residues belonging to the transmembrane domains 3 and 6, *i.e.* Asp^{3.32}, Ser^{3.36}, Phe^{6.52}, and Asn^{6.55}, make direct contacts with 5-HT. In addition, Trp^{3.28}, Phe^{3.35}, Phe^{6.52}, and Phe^{7.38} form an aromatic box surrounding 5-HT. The specificity of human and mouse 5-HT_{2B}Rs may be reflected by different rearrangements of the aromatic network upon 5-HT binding. Two amino acids close to Pro^{5.50} in the human transmembrane domain 5 sequence were permuted to introduce a “mouse-like” sequence. This change was enough to confer the human 5-HT_{2B}R properties similar to those of the mouse. Taken together, the computed models and the site-directed mutagenesis experiments give a structural explanation to (i) the different 5-HT pK_D values measured with the human and mouse 5-HT_{2B}Rs (7.9 and 5.8, respectively) and (ii) the specificity of 5-HT binding to 5-HT_{2B}Rs as compared with other serotonergic G-protein coupled receptors.

rat (2), mouse (3), and human (4) 5-HT_{2B} receptors (5-HT_{2B}Rs) are highly similar at the level of the predicted transmembrane domains (TMDs); they exhibit 88, 82, and 79% homology upon comparison of mouse and rat, human and mouse, and human and rat receptors, respectively (5). Moreover, significant correlations were established between the pharmacological profiles of human and rat (or human and mouse) 5-HT_{2B}Rs but not between those of mouse and rat (5). Nevertheless, some compounds (*e.g.* certain ergolines and benzoylpiperidines) can be used to discriminate pharmacologically between human and rat 5-HT_{2B}Rs (6).

Structural descriptions of these receptors and of their binding interactions are required to rationalize the above findings. In the absence of any 5-HT receptor three-dimensional structure, computer modeling studies were undertaken in the present study. Our aim was to explain the different 5-HT pK_D values measured for the rat, mouse, and human 5-HT_{2B}Rs (7.5, 5.8, and 7.9, respectively) and to better understand the mechanism of 5-HT_{2B}R activation.

Two main strategies have already been used to build GPCR three-dimensional models. The first one relied on the use of the structure of bacteriorhodopsin (BR) at a 3-Å resolution as a homology template (7, 8). The second strategy, already used for three-dimensional modeling of the 5-HT_{2A} (9, 10) and 5-HT_{2C} receptors (10, 11), aimed at constructing models *de novo* by only using the ~9-Å structure of bovine rhodopsin (RH) as a guide to orient the TMDs. These studies were the starting point in the elucidation of the conformational switch between the inactive and active states of GPCRs. A key feature of these approaches involved the replacement of the network of constraints in the inactive ground state of the receptor by a ligand-induced set of interactions in the activated state (12–14).

In the present work, the construction of three-dimensional models of the mouse and human 5-HT_{2B}Rs was carried out using either the high resolution BR structure (15, 16) as templates. Structural models of the native receptors liganded or not with 5-HT could be derived. In a second step, site-directed mutagenesis experiments were performed to validate the models. Residues predicted to participate to 5-HT binding in either the human or the mouse 5HT_{2B}R were changed. 5-HT binding affinity and 5-HT-induced inositol triphosphate (IP₃) production were systematically assessed with each mutated receptor. As a result, the involvement in 5-HT binding of several amino acid residues could be established. Moreover, a two-amino acid permutation in the TMD5 of the human receptor was performed to introduce a mouse-like sequence. This modification

Of the 14 mammalian serotonin (5-hydroxytryptamine (5-HT)¹) receptor subtypes, all but one (5-HT₃) belong to the super-family of G-protein-coupled receptors (GPCRs) (1). The 5-HT₂ subtype comprises three closely related receptors, which are 5-HT_{2A}, 5-HT_{2B}, and 5-HT_{2C}. Amino acid sequences of the

* The costs of publication of this article were defrayed in part by the payment of page charges. This article must therefore be hereby marked “advertisement” in accordance with 18 U.S.C. Section 1734 solely to indicate this fact.

^{‡‡} To whom correspondence should be addressed: Service de Biochimie, Hôpital Lariboisière, 2 rue Ambroise Paré, 75475 Paris cedex 10, France. Tel.: 33-1-49-95-64-33; Fax: 33-1-49-95-84-77; E-mail: jean-marie.launay@rb.ap-hop-paris.fr.

¹ The abbreviations used are: 5-HT, serotonin; 5-HT_{2B}R, serotonin-2B receptor; BR, bacteriorhodopsin; GPCR, G-protein-coupled receptor; IP₃, inositol trisphosphate; MD, molecular dynamics; RH, rhodopsin; r.m.s.d., root mean square deviation; TMD, trans-membrane domain; ALF, fluorescent sequencing system.

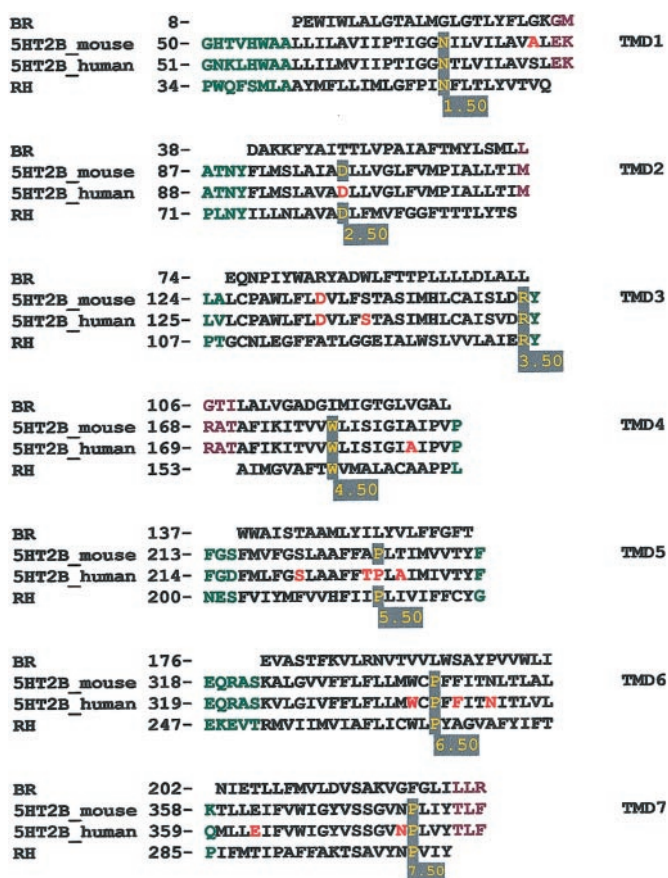


FIG. 1. Amino acid sequence alignment of BR, RH, and mouse and human 5-HT_{2B} TMDs. Each helix amino terminus starting residue is numbered according to SWISSPROT data bank sequences (BR, P02945; mouse 5-HT_{2B} receptor, Q02152; human 5-HT_{2B} receptor, P41595; RH, P02699). In addition, a consensus numbering scheme (Ref. 20; see "Experimental Procedures"), referring to the most conserved residue (shown in yellow and shaded in gray) of each TMD among the GPCR superfamily, was used. BR- and RH-specific sequences used as structural templates are shown in green and purple, respectively. Amino acid residues subjected to site-directed mutagenesis are shown in red.

resulted in a lowering of the 5-HT affinity and in a change of the IP₃ production to values similar to those measured with the mouse 5-HT_{2B}R. We conclude that the TMD5 region encompassing the mutated residues participates in the species signature of the 5-HT_{2B}Rs.

EXPERIMENTAL PROCEDURES

Molecular Modeling—Three-dimensional models of the TMD bundle of the human and mouse 5-HT_{2B}Rs were built using criteria and procedures that took into account sequence conservation (17, 18) and degree of residue polarity (19) and incorporated a large number of experimental constraints as reviewed elsewhere (20). Constraints related to 5-HT₂ receptors (21) were particularly considered; for instance, in the prediction of TMD boundaries, occurrence of an Arg/Lys motif at the cytoplasmic side was imposed.

Residues in the receptor sequences are numbered according to Ballasteros and Weinstein (20). Briefly, for example, residues of TMD3 are numbered with reference to the arginine at the bottom of the helix, which is the most conserved amino acid in this helix (Fig. 1). The arginine locus is thus designated 3.50. Adjacent residues are 3.49 and 3.51. A number in parentheses is also associated to each residue. It corresponds to the standard amino-terminal based numbering. Another example is the TMD3 aspartate, which is conserved among neurotransmitter receptors; it will be designated Asp^{3.32(h135)} in the murine 5-HT_{2B} receptor, Asp^{3.32(h135)} in the human 5-HT_{2B} receptor (because of an additional amino acid at the 10th position in the human 5-HT_{2B} receptor sequence), and Asp^{3.32(h135,m134)} when reference will be made to both receptors. All the bioamine-GPCR sequences presently available

were aligned with BR and RH using the CLUSTAL X software (22). For clarity, only the TMD sequences of the two templates and of the two studied 5-HT_{2B}Rs are presented in Fig. 1.

Model refinements, energy minimization, and molecular dynamics (MD) simulations were performed with the CHARMM program (23). A 20-Å cut-off was applied to non-bonded interactions. All graphical manipulations used a Silicon Graphics O₂ station with the Insight II modeling package (Molecular Simulations Inc., San Diego, CA). Calculations were performed on a cluster of PC computers running under a Linux operating system.

To minimize errors inherent to the generation of receptor three-dimensional models, 10 BR-based and 10 RH-based models were generated for each 5-HT_{2B}R, leading to 40 receptor models. The two sets of models were built on the basis of the backbone coordinates of 1BRD (24) and 1HZX (16) files from the Protein Data Bank. Side chains of the mouse and human 5-HT_{2B}Rs were positioned using the Biopolymer module of Insight II software. Interhelix contacts were adjusted by taking into account data from site-directed mutagenesis experiments. After 800 ps of constrained MD simulations, average structures resulting from 200 ps of free MD simulations were energy-minimized. The obtained relaxed and equilibrated receptors were further used for the docking of 5-HT.

5-HT was modeled in its cationic (protonated) state, the major entity at physiological pH (25). To check the accuracy of the 5-HT empirical force-field parameters, a conformational analysis was performed on the side chain of the 5-HT molecule with the CHARMM force field. The α and β dihedral angles of the ligand were varied from 0° to 360° by 30° increments. Six energy minima (conformers) were deduced (data not shown). The corresponding relative free energies are in satisfactory agreement with those of the conformers obtained from semi-empirical (Intermediate Neglect Differential Overlap and Perturbative Configuration Interaction using Localized Orbitals) calculations (26).

Docking of 5-HT to the 40 obtained receptor models was performed in the vicinity of the negatively charged residues located at the inward face of the receptors (Asp^{2.50(h100,m99)}, Asp^{3.32(h135,m134)}, and Glu^{7.36(h363,m362)}). Different initial orientations were assayed. Simulations of the ligand/receptor complexes were carried out in three steps, which are 50 ps at 10 K, 50 ps at 310 K, and 200 ps at 310 K. Equilibrated structures of ligand-receptor complexes were obtained by averaging the energy-minimized structures over the third simulation period.

Point mutations were introduced in the models of the mouse and human 5-HT_{2B}Rs by replacing the side chain of a wild-type residue. The positioning of each mutated residue was optimized as for the wild-type receptor. All atoms of the receptor were held fixed except those of the mutated residue, and a short minimization step was applied. The receptor atom coordinates were then allowed to relax. Ligand docking to the variant receptors and simulations of the ligand/receptor complexes were performed as above. Conformational stability likelihood of the generated 5-HT_{2B}R models were systematically assessed by following the root mean square deviations (r.m.s.d.) of the Cartesian coordinates of the backbone atoms at all steps of the simulations.

Site-directed Mutagenesis—Full coding regions of the human or mouse 5-HT_{2B}R cDNAs (3, 4) were subcloned in the mammalian expression vector pRC/CMV (Invitrogen). Mutations were introduced using the QuikChange site-directed mutagenesis kit (Stratagene) and verified by DNA sequencing with an automated fluorescent sequencing system (ALF, Amersham Biosciences).

Cellular Expression—To analyze the pharmacological and functional profiles of the engineered receptors, wild-type or mutated cDNAs were stably transfected in LMTK⁻ cells (27). To avoid transcriptional bias at the level of the expression of the 5-HT_{2B}R variants, cell lines expressing comparable amounts of RNA from cDNA were selected by Taqman analysis. Because mutations may interfere with the cellular localization of 5-HT_{2B}Rs despite roughly similar mRNA levels, the relative amounts of receptors expressed at the cell surface were also estimated. Such measurements involved comparisons of maximal cellular 5-HT binding capacities (B_{max}).

Ligand Binding and Coupling Assays—Pharmacological and functional properties of the various mutated 5-HT_{2B}Rs were compared with those of the human or mouse wild-type receptors through determination of (i) their 5-HT binding affinity (K_D) and maximal 5-HT binding capacity (B_{max}) and (ii) their transduction efficacy as characterized by both the maximal 5-HT-induced IP₃ production (E_{max}) and the 5-HT concentration eliciting a half-maximal IP₃ response (EC_{50}). Ligand binding analyses were performed as described by Wainscott *et al.* (6). Briefly, binding experiments were carried out with cell membranes in 1 ml, incubated at 37 °C under shaking. Assays were initiated by the

TABLE I
r.m.s.d. of the backbone atoms of each form of the 5-HT_{2B}R models

Unliganded forms were averaged after 10 runs of 600 ps of constrained MD simulations (the reference structures were the energy-minimized starting structures) and after 50–200 ps of free MD simulations (the reference structures were those issued from constrained MD simulations). Liganded forms were averaged after 10 runs of 50 ps of preparative MD simulations at 10 K (the reference structures were the energy-minimized starting structures), after 50 ps of 310 K MD simulations (the reference structures were those issued from 10 K MD simulations), and after 100–200 ps of 310 K MD simulations (the reference structures were those issued from the first 50 ps of 310 K MD simulations).

Three-dimensional models		Unliganded		Liganded		
		Constrained MD	Free MD	50 ps 10 K MD	50 ps 310 K MD	100–200 ps 310 K MD
BR-like models	Mouse	4.0 ± 0.5	0.7 ± 0.2	0.8 ± 0.2	1.9 ± 0.5	1.0 ± 0.2
	Human	3.0 ± 0.3	1.7 ± 0.2 ^a	1.3 ± 0.3	3.0 ± 0.4	1.9 ± 0.2 ^a
RH-like models	Mouse	3.0 ± 0.2	1.1 ± 0.2	1.1 ± 0.3	3.0 ± 0.3	1.1 ± 0.1
	Human	3.2 ± 0.2	1.2 ± 0.3	1.4 ± 0.2	3.0 ± 0.2	1.2 ± 0.2

^a Significant ($p < 0.05$) difference between the human and the mouse 5-HT_{2B}R models.

addition of 100 μ l of fetal calf serum-free Dulbecco's modified Eagle's medium supplemented with 2 nM [³H]5-HT and various concentrations of unlabeled 5-HT. After a 15-min incubation, cells were washed twice with cold Dulbecco's modified Eagle's medium and 2 ml of 1 N HClO₄ were added. Radioactivity was counted in a 500- μ l fraction using a liquid scintillation counter (Packard Instrument Co.). The specific binding (mean 38%) corresponded to the difference observed in the absence and presence of 10 μ M unlabeled 5-HT. The 5-HT-induced IP₃ amounts produced by the cells were measured as described previously (27). Data were analyzed using the iterative non-linear regression fitting program Ligand (version 3.0) and RS/1 (release 4.0).

RESULTS

Computer Modeling of Human and Mouse Wild-type 5-HT_{2B} Receptors—As a first step, the seven TMDs of the 5-HT_{2B}R models were organized in a counterclockwise arrangement. In the case of the RH-based modeling, constraints resulting from the alignment of the 5-HT receptor sequences to the template led to an electrostatic interaction between Asp^{2.50(h100,m99)} and Asn^{7.49(h376,m375)}. This interaction was already evidenced between Asp^{2.50(120)} and Asn^{7.49(396)} in the human 5HT_{2A}R (28). With the BR-based models, the orientation of TMD7 with respect to TMD2 had to be slightly modified to establish a similar interaction between Asp^{2.50(h100,m99)} and Asn^{7.49(h376,m375)}. By introducing this constraint in the BR-based models, 8 of the 10 starting low energy structures could be retained (see "Experimental Procedures"). However, in these structures, Glu^{7.36(h363,m362)} now faced the phospholipid bilayer instead of the inward face of the receptor. We thus rotated TMD7 to point Glu^{7.36(h363,m362)} toward the central core of the receptors. Such a rotation, which slightly moved Asn^{7.49(h376,m375)} away from Asp^{2.50(h100,m99)}, allowed Glu^{7.36(h363,m362)} to interact directly with 5-HT in the BR-based models (see below). Asp^{2.50(h100,m99)} also interacted with Asn^{1.50(h72,m71)} via a hydrogen bond network in both the BR- and RH-based models of 5-HT_{2B}Rs. The resulting H-bond network conferred stability to the packing of TMDs 1, 2, and 7.

For all the 5-HT_{2B}R models, large conformational changes occurred during the first phase of constrained MD simulations (Table I). This step allowed the major van der Waals clashes to vanish and the models to gently evolve toward relaxed structures. After 200 ps of free MD simulations, the structures of the generated 5-HT_{2B}Rs reached stability. The r.m.s.d. of the backbone atom coordinates remained constant for all models after 100 ps of free MD simulations. By considering all models, TMDs could be classified into two sets, TMDs 1, 2, 3, and 4 associated to low r.m.s.d. (0.6 ± 0.2 Å) and TMDs 5, 6, and 7 with higher r.m.s.d. (1.4 ± 0.3 Å).

Docking of 5-HT to Human and Mouse Wild-type 5-HT_{2B} Receptors—In the presence of 5-HT, significant conformational changes occurred during the first 50 ps of the 310 K MD simulations. Relaxed structures were obtained after 100 ps. The low r.m.s.d. values obtained during the preparative 10 K MD phase are likely to reflect the low temperature used. Similarly to what

was observed with the unliganded receptors, motions of TMDs 5 and 6 and, to a lesser extent, TMD7, mainly contributed to the observed r.m.s.d. in the liganded receptors (Table I).

Whatever the template used, a strong electrostatic interaction formed in the course of all simulations between the cationic amino group of 5-HT and the carboxylate group of Asp^{3.32(h135,m134)}. This observation supports the primordial importance of Asp^{3.32} as the major counterion for 5-HT binding to 5-HT₂Rs (21).

In 5-HT_{2B}R BR-based models (Figs. 2, *c* and *d*, and 3, *b* and *d*), the 5-HT amino group also interacted with Asn^{6.55(h344,m343)} and Phe^{6.52(h341,m340)}. Moreover, the hydroxyl group of Ser^{3.36(h139,m138)} was forced to point toward the 5-hydroxyl group of 5-HT rather than toward the carboxyl group of Asp^{3.32(h135,m134)}. Upon 5-HT binding, rotation of the Phe^{6.52(h341,m340)} aromatic ring affected the aromatic network within the hydrophobic pocket delimited by TMDs 4, 5, 6, and 7. The two contacted aromatic residues, Phe^{6.52(h341,m340)} and Trp^{6.48(h337,m336)}, adopted a "T-shape"-oriented structure. With human and mouse 5-HT_{2B}Rs, 5-HT also establishes van der Waals contacts with Trp^{3.28(h131,m130)} and Leu^{7.35(h362,m361)}. Additional contacts were with Phe^{3.35(138)} and Phe^{7.38(365)}, in the case of the human 5-HT_{2B}R, and with Lys^{7.32(358)} and Val^{7.39(365)}, in the case of the mouse 5-HT_{2B}R. Thus, the 5-HT binding sites in the human and mouse 5-HT_{2B}R BR-based models involve TMDs 3, 6, and 7. However, 5-HT appeared more closely packed with TMD3 in the human receptor than in the mouse. This difference is likely to result from stronger hydrogen bonding between the indolic NH group of 5-HT and Glu^{7.36(h363,m362)} in the mouse 5-HT_{2B}R. As a consequence, the interaction between the hydroxyl group of 5-HT and the OH group of Ser^{3.36(h139,m138)} would be weakened.

In the course of MD simulations of the RH-based models (Figs. 2, *a* and *b*, and 3, *a* and *c*), we also noticed that the 5-HT cationic amino group interacted with the carboxylic group of Asp^{3.32(h135,m134)} and that the 5-HT hydroxyl group was H-bonded by the OH group of Ser^{3.36(h139,m138)}. These features could also be observed in the BR-based models. However, in the RH-based models, the carbonyl group of Asn^{6.55(h344,m343)} no longer interacted with the cationic amino group of 5-HT. Rather, it interacted weakly with the 5-HT indolic NH group. During the simulations, the 5-HT molecule moved toward TMDs 6 and 7. This translation was more pronounced in the case of the human 5-HT_{2B}R than in the case of the mouse receptor. The relative TMD motions in the 5-HT_{2B}R RH-based models were similar to those in the BR-based models. In particular, r.m.s.d. values were larger for TMD5 and -6 backbone atoms. In both BR- and RH-based models complexed with 5-HT, motions of proline residues belonging to TMDs 5 and 6 accompanied the rearrangement of the hydrophobic pocket including Trp^{6.48(h337,m336)} and Phe^{6.52(h341,m340)}. Motions of Phe^{6.52(h341,m340)} and Trp^{6.48(h337,m336)} also accompanied the

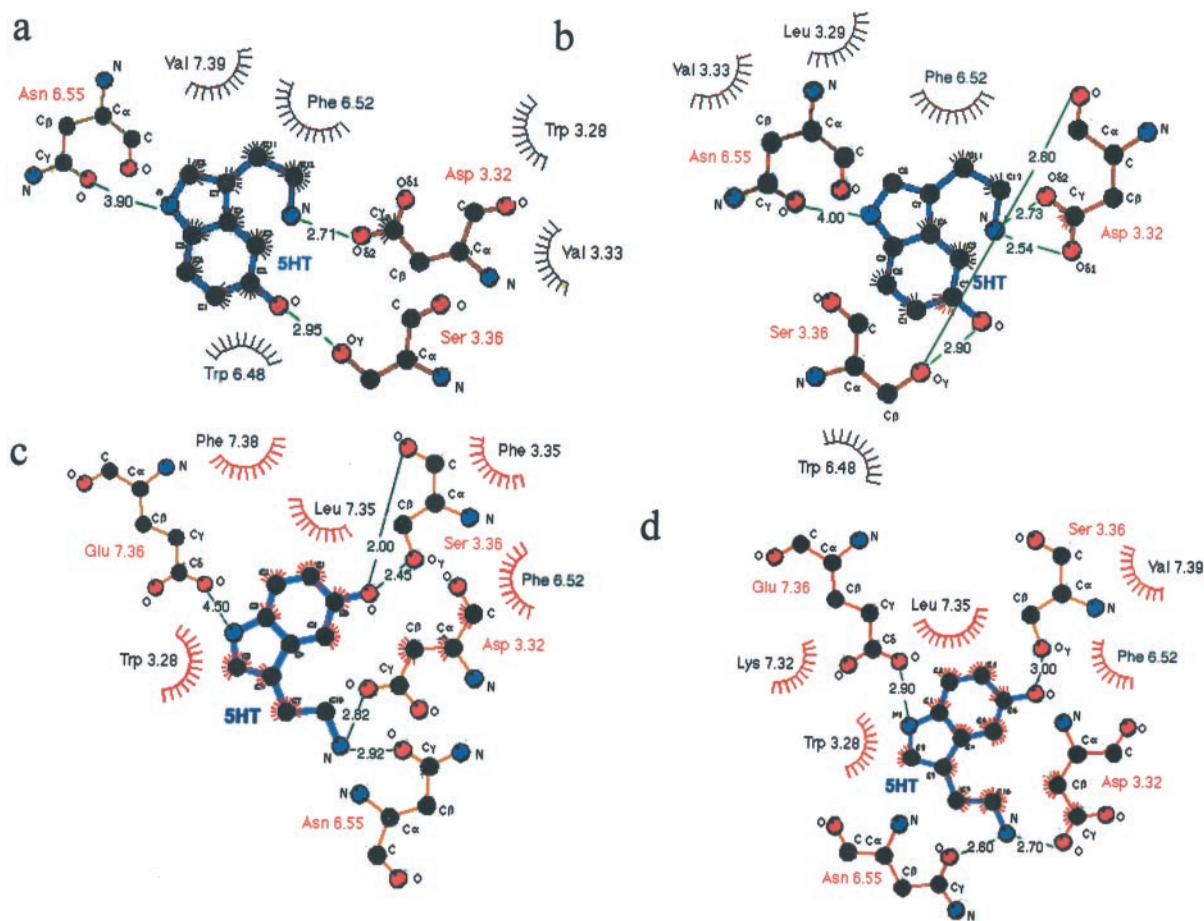


FIG. 2. Two-dimensional views of 5-HT docked to RH (a and b)- and BR (c and d)-based three-dimensional models of human (a and c) and mouse (b and d) 5-HT_{2B} receptors. Amino acids in ball and stick models are those that make electrostatic interactions with 5-HT. Trp^{3.28}, Trp^{6.48}, and Phe^{6.52} participate to the aromatic environment surrounding 5-HT. Predicted H bonds are depicted as green lines.

5-HT translation. This motion had, however, a smaller amplitude with the mouse 5-HT_{2B}R than with the human. After completion of the MD simulations with the eight low energy structures previously selected, (i) the 5-HT cationic group still interacted with Asp^{3.32(h135,m134)}, (ii) the 5-HT hydroxyl group was H-bonded to the hydroxyl group of Ser^{3.36(h139,m138)}, and (iii) new van der Waals contacts formed between 5-HT and Val^{3.33(h136,m135)} in the case of both receptors, between 5-HT and Leu^{3.29(m131)} with mouse, and between 5-HT and Trp^{3.28(h131)} plus Val^{7.39(h366)} with human. In the two receptors, the 5-HT indolic NH group still pointed toward the oxygen atom of Asn^{6.55(h344,m343)}. However, the resulting electrostatic bond appeared weaker with the human receptor, because of the relatively large translation of 5-HT toward TMDs 6 and 7. This difference may reflect the different sets of van der Waals contacts observed in the liganded human and mouse 5-HT_{2B}Rs. Thus, similarly to the BR-based models, 5-HT binding to the human and mouse RH-based 5-HT_{2B}R models involve TMDs 3, 6, and 7. Nevertheless, interactions involving TMD7 are fainter in the RH-based models than in those BR-based.

Functional Analysis of Human and Mouse Mutant 5-HT_{2B} Receptors—Three-dimensional modeling of the human and mouse 5-HT_{2B}Rs suggests that 5-HT binding relies on a limited number of residues. To assess the contribution of these amino acids to the species-specific pharmacology of 5-HT_{2B}Rs, mutant receptors were engineered by site-directed mutagenesis. The 5-HT binding properties (K_D , B_{max}) and the 5-HT-induced efficacy (EC_{50} and E_{max} of IP₃ production) were measured in stably transfected LMTK⁻ cells expressing variant receptors (Table

II). Cells transfected with the corresponding wild-type receptor were used for comparison. To avoid transcriptional variations between cell strains, clones expressing comparable amounts of 5-HT_{2B}R mRNA were selected by Taqman analysis and used in further biochemical and pharmacological experiments.

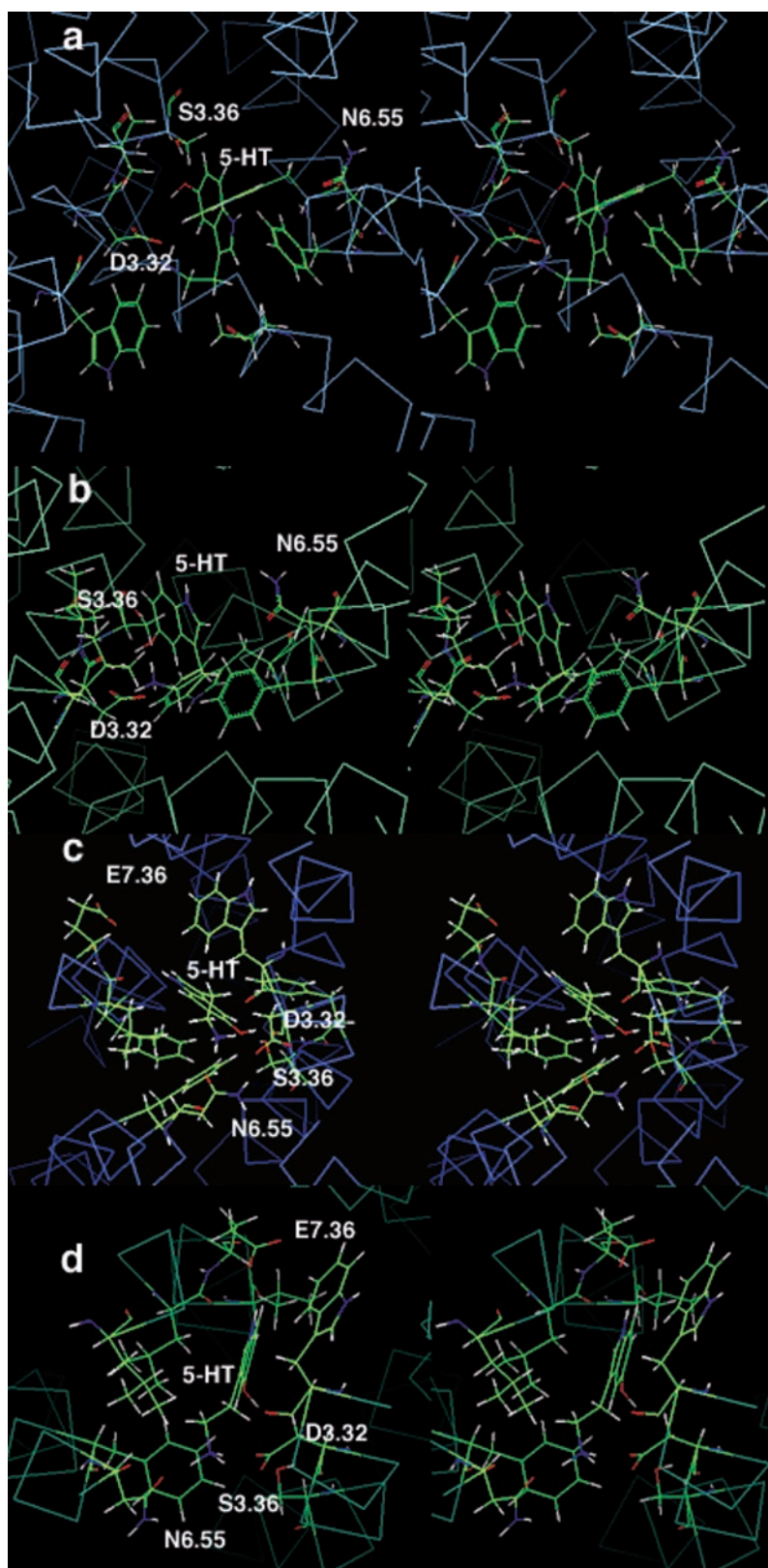
D135A Human and D134A Mouse 5-HT_{2B}Rs—In the 5-HT_{2B}R (BR- or RH-based) models, Asp^{3.32(h135,m134)} side chain acts as the primary counterion of the protonated amino group of 5-HT. The D(h135,m134)A mutation in the two 5-HT_{2B}R sequences (human and mouse) markedly decreased both the 5-HT binding affinity and the transduction efficacy.

S139A Human 5-HT_{2B}R—Ser^{3.36(h139)} was predicted to be involved in 5-HT binding in both the BR- and the RH-based models. The S139A mutation affected neither the receptor expression level (B_{max}) nor the maximal 5-HT-induced IP₃ production (E_{max}), whereas the binding affinity for 5-HT was reduced about 30-fold. Such a factor underlines the crucial role of Ser-139 in 5-HT binding.

N344A, S222A, and S222A/N344A Human 5-HT_{2B}R—In either the BR- or the RH-based models of 5-HT_{2B}Rs, Asn^{6.55(h344)} was suspected to directly interact with 5-HT. In agreement with this prediction, substitution of this residue by Ala in the human receptor led to a decrease (7-fold) of the 5-HT binding affinity. Other assayed properties of the receptor remained unchanged.

Ser^{5.43(h222,m221)}, a conserved residue in the 5-HT_{2R} family (21), is likely to be involved in the H-bonding of the 5-HT hydroxyl group. Surprisingly, the S222A mutation did not interfere either with the 5-HT binding affinity or with the IP₃

FIG. 3. Stereoview of the 5-HT molecule in the binding site of RH (*a* and *c*)- and BR (*b* and *d*)-based models of human (*a* and *b*) and mouse (*c* and *d*) 5-HT_{2B} receptors. 5-HT is at the center of the binding pocket of the 5-HT_{2B} receptors. D3.32 (Asp^{3.32(h135,m134)}) is the primary counter-ion that interacts with the 5-HT amino group. S3.36 (Ser^{3.36(h139,m138)}) H binds the OH group of 5-HT. N6.55 (Asn^{6.55(h344,m343)}) stabilizes 5-HT in its binding pocket through interactions with either the indole ring or the amino group of the neurotransmitter depending on the template used for the modeling. Note the larger 5-HT binding site in the human 5-HT_{2B} receptor (*a* and *b*) than in the mouse (*c* and *d*).



production. It only induced a 2-fold decrease of the expression level of the receptor. These results bring support to the BR-based models of the human receptor. In our models, TMDs 3 and 5 together have no probability to H-bond 5-HT. Indeed, the distance between the center of mass of 5-HT and the OH group of Ser^{5.43(h222)} appears too large (15.5 Å). Therefore, Ser^{3.36(h139,m138)} instead Ser^{5.43(h222,m221)} is likely to contact the OH group of the neurotransmitter.

It is of note that structure-function studies based on mutagenesis experiments of a single residue followed by functional analyses, such as the measurement of the affinity of a single ligand, cannot distinguish between either a modification of contacts between the receptor and the ligand or conformational changes within the overall receptor structure. Thus, because Asn^{6.55(h344)} might compensate for the loss of Ser^{5.43(h222)} in the RH-based 5-HT_{2B}R models, we decided to engineer the double

TABLE II

5-HT binding characteristics and 5-HT-induced IP₃ production in LMTK⁻ cells stably transfected by wild-type or mutant 5-HT_{2B} receptors

Binding data are defined through 5-HT binding dissociation constants (K_D) and maximal 5-HT binding capacities (B_{\max}). The transduction efficacies are expressed by both the maximal 5-HT-induced IP₃ productions (E_{\max}) and the 5-HT concentrations eliciting a half-maximal IP₃ response (EC_{50}) (see "Experimental Procedures"). Each value is the mean (\pm S.E.) of three to five independent experiments performed in triplicate. ND, not determined.

5-HT _{2B} receptors	K_D	B_{\max}	EC_{50}	E_{\max}
	nM	fmol/mg protein	nM	fmol/mg protein
Wild-type				
Mouse	1,445 \pm 141 ^a	408 \pm 48	676 \pm 41 ^a	761 \pm 64
Human	12 \pm 2 ^b	392 \pm 39	9 \pm 1 ^b	804 \pm 58
Mutant				
TMD1				
Mouse A79S	1,514 \pm 170 ^a	396 \pm 28	794 \pm 52 ^a	792 \pm 46
TMD2				
Human D100N	148 \pm 15 ^{a,b}	441 \pm 38	120 \pm 12 ^{a,b}	364 \pm 82 ^{a,b}
TMD3				
Mouse D134A	>10,000 ^{a,b}	ND	>10,000 ^{a,b}	ND
Human D135A	>10,000 ^{a,b}	ND	>10,000 ^{a,b}	ND
Human S139A	347 \pm 13 ^{a,b}	423 \pm 46	17 \pm 1 ^{a,b}	787 \pm 88
TMD4				
Human A187S	9 \pm 1 ^b	211 \pm 16 ^{a,b}	9 \pm 1 ^b	806 \pm 76
TMD5				
Human S222A	11 \pm 2 ^b	189 \pm 19 ^{a,b}	11 \pm 1 ^b	794 \pm 71
Human T228A	1,096 \pm 169 ^a	398 \pm 32	186 \pm 12 ^{a,b}	168 \pm 37 ^{a,b}
Human P229A	10 \pm 2 ^b	200 \pm 19 ^{a,b}	7 \pm 1 ^b	814 \pm 48
Human A231T	93 \pm 16 ^{a,b}	368 \pm 32	56 \pm 15 ^{a,b}	181 \pm 27 ^{a,b}
Human T228A + A231T	1,230 \pm 14 ^a	394 \pm 45	795 \pm 51 ^a	152 \pm 17 ^{a,b}
TMD6				
Human W337A	132 \pm 16 ^{a,b}	344 \pm 26	13 \pm 1 ^b	788 \pm 80
Human F341A	174 \pm 13 ^{a,b}	422 \pm 37	14 \pm 1 ^b	786 \pm 81
Human N344A	83 \pm 15 ^{a,b}	354 \pm 28	13 \pm 2 ^b	787 \pm 82
TMD7				
Human E363A	58 \pm 15 ^{a,b}	181 \pm 18 ^{a,b}	11 \pm 1 ^b	796 \pm 76
Human N376D	141 \pm 16 ^{a,b}	342 \pm 25	120 \pm 13 ^{a,b}	296 \pm 39 ^{a,b}
TMDs 2 + 7: human D100N/N376D	14 \pm 2 ^b	394 \pm 47	11 \pm 1 ^b	794 \pm 59
TMDs 5 + 6: human S222A/N344A	85 \pm 14 ^{a,b}	353 \pm 36	10 \pm 1 ^b	798 \pm 78

^a Significant ($p < 0.05$) difference *vs.* the human wild-type receptor.

^b Significant ($p < 0.05$) difference *vs.* the mouse wild-type receptor.

mutant S222A/N344A. With this mutant, the decrease in 5-HT affinity was of similar magnitude than that observed with the N344A single mutant. This result strengthens the idea that Ser^{5.43(h222)} has no direct role in the binding of 5-HT to the human 5-HT_{2B}R.

W337A and F341A Human 5-HT_{2B}Rs—The aromatic residues Trp^{6.48(h337)} and Phe^{6.52(h341)} were also predicted to be involved in 5-HT binding and/or IP₃ production. Mutation of any of these residues significantly decreased (11–15-fold) the binding affinity of 5-HT. In contrast, the receptor expression level and the 5-HT-induced IP₃ synthesis remained insensitive to the mutations.

D100N, N376D, and D100N/N376D Human 5-HT_{2B}Rs—Mutations of either Asp^{2.50(100)} or Asn^{7.49(376)} did not affect the receptor expression. However, the 5-HT affinity was decreased by 12-fold, and the maximal 5-HT-induced IP₃ production was reduced by 2.5-fold. These effects disappeared upon construction of the double mutant receptor D100N/N376D. Such results nicely illustrate the electrostatic interaction established between these two amino acids. We may therefore conclude that whatever the template (BR or RH) used, the interaction between TMDs 2 and 7 is of crucial importance for 5-HT binding and 5-HT-induced IP₃ production.

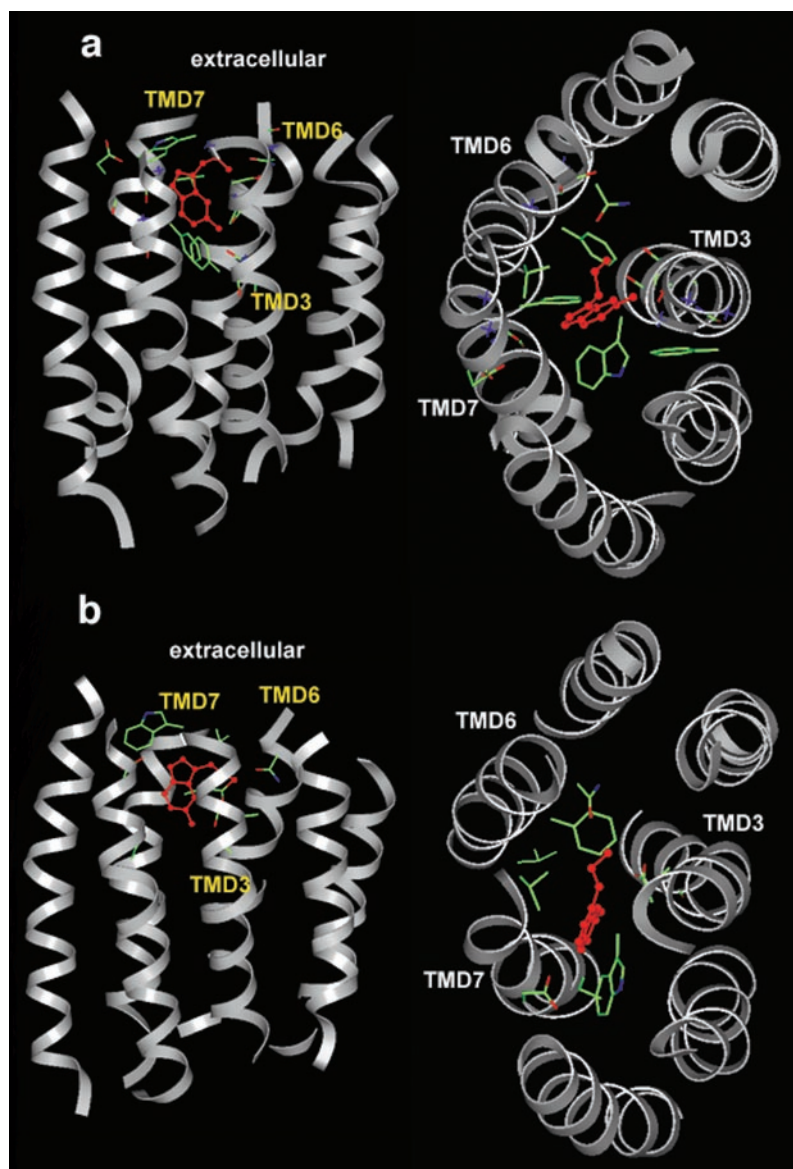
E363A Human 5-HT_{2B}R—Only in the BR-based models of 5-HT_{2B}Rs, Glu^{7.36(363)} seems to be involved in 5-HT binding. Through rotation of TMD7, Asn^{7.49(376)} and Asp^{2.50(100)} can be allowed to interact with the side chain of the Glu^{7.36(363)} residue, which points toward the inward face of the receptor. However, because Asn^{7.49(376)} and Glu^{7.36(363)} are separated by almost a helix half-turn, the interaction between Glu^{7.36(363)} and the indolic NH group of 5-HT should be relatively weak. Indeed, the amplitude of the decreases in both the expression

level (2-fold) and the 5-HT binding affinity (5-fold) of the E363A mutant remained modest.

A187S Human 5-HT_{2B}R—A serine is conserved at the 4.57 locus of all GPCRs except 5-HT_{2B}Rs in which an alanine is present. In a RH-based model of 5-HT_{2A}R, Ser^{4.57(207)} was reported to form a hydrogen bond with the NH indolic group of 5-HT (26). According to our RH-based models of 5-HT_{2B}R, an A187S substitution should restore the H-bond interaction with this indolic group. Such a change should also reinforce the interaction of the 5-HT hydroxyl group with Ser^{5.43(h222)} and disrupt the contact between 5-HT and Asn^{6.55(h344)}, a residue involved in the binding site. In contrast, in our BR-based models of the human 5-HT_{2B}R-A187S mutant, the H-bond between the NH indolic group of 5-HT and the substituted Ser does not occur. Actually, no variation of either 5-HT binding affinity or the IP₃-induced efficacy could be detected with the A187S mutant if compared with the wild-type receptor. The mutation only reduced the expression level by 2-fold (Table II).

A79S Mouse 5-HT_{2B}R—Among the 6 "mouse-specific" (*versus* human and rat 5-HT_{2B}R sequences) TMD residues (Ala^{1.58(m79)}, Ile^{2.48(m97)}, Val^{5.40(m218)}, Ala^{6.36(m324)}, Val^{6.39(m327)}, and Leu^{6.56(m344)}, Fig. 1), Ala^{1.58} replaces a Ser residue present in all other members of the 5-HT₂R family including human and rat 5-HT_{2B}Rs. Therefore, this residue is susceptible to account for the loss of a hydrogen bond in the complex of 5-HT with the mouse receptor. This loss would explain the low affinity of 5-HT for the mouse 5-HT_{2B}R. However, mouse wild-type and A79S 5HT_{2B}Rs displayed similar 5-HT bindings and transduction efficacies (Table II). Therefore, an involvement of Ala^{1.58(m79)} in 5-HT binding can be rejected. This conclusion is in agreement with the excessive distance between this TMD1 residue and the 5-HT molecule (8 Å be-

FIG. 4. Proposed transmembrane domain arrangements of BR-based models of human (a) and mouse (b) 5-HT_{2B} receptors liganded with 5-HT.



tween the indolic nitrogen atom of 5-HT and the C β of Ala^{1.58(m79)}. Ala^{1.58(m79)} should not, therefore, participate to the mouse *versus* human 5-HT binding specificity.

T228A, P229A, A231T, and T228A/A231T Human 5-HT_{2B}Rs—Significant differences in r.m.s.d. values between human and mouse 5-HT_{2B}R models, liganded or unliganded, could only be evidenced in the cases of the BR-based structures (Table I). Divergences in r.m.s.d. were observed mainly at the level of TMDs 5 and 6. We hypothesized that differences in the motions of these helices reflect their amino acid composition, in particular at the level of the amino acids in the vicinity of the Pro residues (29, 30). Bearing in mind that standard MD simulation algorithms do not allow simulations of the protein folding processes and that r.m.s.d. differences between human and mouse 5-HT_{2B}Rs were not so large, we mutated Thr^{5.49(228)} and Ala^{5.52(231)} adjacent to Pro^{5.50(229)} in TMD5 of the human 5-HT_{2B}R. The aim of this construction was to create a mouse-like sequence in this region (Fig. 1). Table II shows the resulting huge decrease (90–100-fold) of both the 5-HT binding affinity and the IP₃-coupling property of the obtained human double mutant receptor T228A/A231T. This mutant now exhibits characteristics similar to that of the mouse receptor with, however, a lower maximal 5-HT-induced IP₃ production (5-fold decrease). Similar effects on the receptor properties were ob-

served with the single T228A (K_D and EC₅₀ values are 90- and 20-fold decreased, respectively) and A231T (a 7-fold factor for both K_D and EC₅₀) mutants. The P229A mutation was also performed. It only induced a 2-fold reduction in the expression level of the receptor. We therefore conclude that the specificities of 5-HT binding by the human or the mouse 5-HT_{2B}R are largely governed by different motions of TMDs 5 and 6.

DISCUSSION

In this report, three-dimensional computer modeling of the TMD bundle of human and mouse 5-HT_{2B}Rs was undertaken on the basis of (i) sequence alignment (17), (ii) fitting to the BR and RH structures, and (iii) side-chain rotamer probability distributions (31). Based on the theoretical models obtained, mutated receptors were expressed and assessed for 5-HT binding affinity and 5-HT-induced IP₃ production. This functional approach allowed us to estimate the relevance of several predictions made on the basis of the sole computations of theoretical models and to propose structural models of 5-HT_{2B}Rs (Figs. 3 and 4). Site-directed mutagenesis experiments also offered the possibility to go deeper into the mechanism of receptor activation (32) by giving particular attention to the conformational switch between the inactive and active states of the receptor. Finally, this work allowed us to define common fea-

tures between receptors of the 5-HT₂ family and to consider the specificity of each 5-HT_{2B}R in their capacity to accommodate the 5-HT ligand.

Modeled 5-HT_{2B}R Structures Share Similarities with Other Members of the 5-HT₂R Family—As previously described in the 5-HT_{2A}R (8, 33, 34) and 5-HT_{2C}R (11) structures, the conserved Asp^{3.32} behaves as the primary counterion for the amino group of 5-HT in human and mouse 5-HT_{2B}Rs. The huge decrease observed upon mutation in both 5-HT binding and signaling efficacy parameters (Table II) confirms its interaction with the agonist in the activated state of the native forms of both human and mouse 5-HT_{2B}Rs.

Undoubtedly, Ser^{3.36(h139,m138)} binds 5-HT in a way similar to that reported for the rat 5-HT_{2C}R (11) and the human 5-HT_{2A}R (9). Substitution of Ser by Ala did significantly decrease the affinity of human 5-HT_{2B}R for 5-HT (Table II). It is likely that Ser^{3.36} stabilizes 5-HT in the receptor binding site by H-bonding through the OH group of the neurotransmitter.

In the rat 5-HT_{2C}R model (11), it was reported that Asn^{6.55} plays a role in the antagonist binding selectivity. In our proposed 5-HT_{2B}R models, Asn^{6.55} is also likely to be involved in 5-HT binding. However, the nature of the interaction between this residue and the neurotransmitter depends on the template used for the modeling.

Despite controversial data in the case of the β₂-adrenergic receptor (35), Asp^{2.50} and Asn^{7.49} were reported crucial for the interaction with most agonist molecules that bind to GPCRs and for the related couplings. This is especially clear with the human 5-HT_{2A}R (28). In 5-HT_{2B}Rs, the 5-HT binding affinity and the signaling efficacy were similarly affected upon introduction of the D100N and N376D mutations. The double conservative mutation D100N/N376D restored the properties of the wild-type receptor (Table II). This behavior strongly indicates that a TMD2/TMD7 helix-helix interaction is required for the human 5-HT_{2B}R to adopt an active conformation.

Originalities of the 5-HT_{2B}R Structural Models—Most of the structural and experimental data collected here suggest that the network of interactions with 5-HT in the 5-HT_{2B}Rs structural models significantly differs from that in 5-HT_{2A/2C}Rs. In particular, the H-bond network that stabilizes 5-HT in the binding site appears characteristic of the 5-HT_{2B}R subtype.

First, the 4.57 locus has unique properties. In the 5-HT_{2A}R, Ser^{4.57} was shown to favor the interaction between 5-HT and Ser^{3.36} by contributing to the formation of a stable complex. In the 5-HT_{2B}R sequence, an Ala residue replaces Ser^{4.57}. This change may explain the rather weak interaction between 5-HT and Ser^{3.36(h139,m138)} in the RH-based models of 5-HT_{2B}Rs. Moreover, in 5-HT_{2B}Rs, none of the residues belonging to TMD4 seem to be involved in the 5-HT binding.

Secondly, the 5-HT hydroxyl group interacts with Ser^{5.43} of rat 5-HT_{2A} (8, 34) and 5-HT_{2C} (11) receptors. RH-based models of 5-HT_{2B}Rs also predicted an H bonding of 5-HT to Ser^{5.43(h222)}. However, this polar interaction could not be evidenced by site-directed mutagenesis (Table II).

Last, the packing of TMDs 1, 2, and 7 in 5-HT_{2B}Rs appears different from that in 5-HT_{2C}R. Indeed, Kristiansen and Dahl (11) report that Asn^{1.50(72)} interacts with both Asp^{2.50(100)} and Asn^{7.49(371)}, whereas in the present models, the interaction involving Asp^{2.50(h100,m99)} and Asn^{7.49(h371,m370)} excludes a participation of Asn^{1.50(h72,m71)}. The TMD2/TMD7 helix-helix interaction in combination with the pointing of the Asn^{7.49(h376,m375)} side chain toward the central core of the receptor allows Glu^{7.36(h363,m362)} to interact with 5-HT. The E363A mutation reduced the ligand affinity without changing the signaling efficacy (Table II). This result indicates that Glu^{7.36(h363,m362)} favors intermolecular contacts with the ligand

in the ground state of the receptor. The presence of a short Asn side chain at locus 7.36 in the other members of the 5-HT₂R family suggests that the longer the side chain of the amino acid at this precise locus, the fewer the interactions between 5-HT, on the one side, and residue 7.36 and TMD2/TMD7, on the other side, can be simultaneously established. Furthermore, MD simulations indicated that the interaction between 5-HT and Glu^{7.36(h363,m362)} is stronger with the mouse than with the human. This result supports the idea of an “easier” mechanism of activation in the case of the human receptor.

The 5-HT_{2B}R Model Validates the “Aromatic Box” Hypothesis—Hibert *et al.* (7) report that the two highly conserved aromatic residues, Trp^{6.48} and Phe^{6.52}, are directly involved in the binding of several neurotransmitters (5-HT, dopamine, and adrenaline) to their corresponding receptors. They also speculate that the side chain conformations of these hydrophobic residues probably changed during the binding process. Such changes could directly affect the conformation of the adjacent helices, in particular in the vicinity of proline residues, and of other helices by propagation along the backbone of interacting conserved aromatic residues. Site-directed mutagenesis experiments also support the crucial role of the two above aromatic residues (36–38).

In all 5-HT GPCRs, six conserved aromatic residues (Trp^{3.28}, Phe^{3.35}, Trp^{4.50}, Phe^{6.44}, Trp^{6.48}, and Trp^{7.40}) are in hydrophobic interaction. In addition, Trp^{3.28}, Phe^{3.35}, Phe^{6.52}, and Phe^{7.38} define an aromatic box that surrounds 5-HT. In our BR-based models of 5-HT_{2B}Rs as well as in models of 5-HT_{2A} and 5-HT_{2C} receptors (21), this box maintains the 5-HT indole ring in a favorable orientation to interact with Asp^{3.32}. The hydrophobic interaction between Phe^{6.52} and the indole ring of 5-HT is crucial for the geometry of the binding cavity. Upon 5-HT binding, a shift of Phe^{6.52(h341)} induces a displacement of the Trp^{6.48(h337)} side chain. Consequently, the other aromatic amino acids in the hydrophobic core of 5-HT_{2B}Rs are submitted to conformational changes. The 5-HT docking also induces van der Waals contacts to occur between Pro^{5.50(h229)} and both the Phe^{6.44(h333)} and Trp^{6.48(h337)} side chains. Such contacts are in agreement with the binding model of 5-HT to the rat 5-HT_{2C}R (11). According to the above observations, mutations of either Phe^{6.52(h341)} and Trp^{6.48(h337)} into Ala decreased by almost 10 times the *K_D* value for 5-HT binding to the human receptor. We conclude that each of these two point mutations affects the ground state of the receptor through rearrangement of the “aromatic network” upon 5-HT binding. Such a rearrangement triggers the switch of the receptor to its active conformation.

Human and Mouse 5-HT_{2B}R Structures Display Distinct Aromatic Boxes—The BR- and RH-derived structural models of the human and mouse 5-HT_{2B}Rs cannot *per se* fully account for the 100-fold difference in 5-HT binding affinity observed between these two receptors. Upon 5-HT binding, as already suggested by Hibert *et al.* (7), the rearrangement of the hydrophobic aromatic core induces proline-mediated motions of TMDs 5 and 6. These motions are of smaller amplitude in the mouse 5-HT_{2B}R model than in the human receptor. Such differences may sustain the species specificity for 5-HT binding. Consistent with this view, simultaneous substitution of Thr^{5.49(h228,m227)} and Ala^{5.52(h231,m230)} on both sides of Pro^{5.50(h229,m228)} in the human sequence by the corresponding residues in the mouse sequence (T228A/A231T) induces a rearrangement of the aromatic network involving 5-HT and the aromatic ring of Phe^{6.52(h341)}. Moreover, our computer modeling strongly indicates that the 5-HT binding pocket in the human receptor, which is larger than that in the mouse, becomes smaller upon these amino acid substitutions. We also noticed that a H bond occurs between the hydroxyl group of

Thr^{5.49(m227)} and the peptidic bond oxygen of Ala^{5.52(m230)}. This intra-helix interaction forms in the course of all MD simulations of the 5-HT/mouse 5-HT_{2B}R complexes. It may provide an explanation for the relatively lower r.m.s.d. values obtained for the mouse 5-HT_{2B}R three-dimensional models. This H bond may reduce the TMD5 motion amplitude and may constrain the aromatic network to accommodate 5-HT at its binding site. Finally, with the human double mutant, both the binding and the signaling parameters reach values similar to those measured with the wild-type mouse 5-HT_{2B}R.

In summary, the present study allowed us to predict that the 5-HT binding site of 5HT_{2B}Rs primarily involves residues belonging to TMDs 3, 6, and 7. The BR-based structures appear more reliable than those RH-based for the modeling of 5-HT_{2B}Rs structures. Indeed, the mutations of residues predicted to be in interaction with 5-HT according to the BR-based models systematically led to relevant results. With the help of site-directed mutagenesis, we show that 5HT_{2B}Rs differ from 5-HT_{2A/2C}Rs and are singular in the 5-HT₂R family. This work also provides a structural basis to explain the difference in 5-HT binding specificity between human and mouse 5-HT_{2B}Rs. In conclusion, the enhanced structural knowledge on 5-HT_{2B}Rs may help in designing specific therapeutic drugs, which may find medical applications in the field of neuroendocrine tumors (39), migraine prophylaxis (40), and dilated cardiomyopathies (41).

Acknowledgments—We thank Professor S. Blanquet for critical reading of the manuscript and very helpful suggestions, Professor M. Hibert for stimulating discussions, Professor H. Weinstein for advice, and Dr. K. Seamans for revision of the manuscript.

REFERENCES

- Hoyer, D., Clarke, D. E., Fozard, J. R., Hartig, P. R., Martin, G. R., Mylecharane, E. J., Saxena, P. R., and Humphrey, P. P. A. (1994) *Pharmacol. Rev.* **46**, 157–203
- Foguet, M., Hoyer, D., Pardo, L. A., Parekh, A., Kluxen, F.-W., Kalkman, H. O., Stühmer, W., and Lübbert, H. (1992) *EMBO J.* **11**, 3481–3487
- Loric, S., Launay, J.-M., Colas, J.-F., and Maroteaux, L. (1992) *FEBS Lett.* **312**, 203–207
- Choi, D.-S., Birraux, G., Launay, J.-M., and Maroteaux, L. (1994) *FEBS Lett.* **352**, 393–399
- Choi, D.-S., Loric, S., Colas, J.-F., Callebert, J., Rosay, P., Kellermann, O., Launay, J.-M., and Maroteaux, L. (1996) *Behav. Brain Res.* **73**, 253–257
- Wainscott, D. B., Lucaites, V. L., Kursar, J. D., Baez, M., and Nelson, D. L. (1996) *J. Pharmacol. Exp. Ther.* **276**, 720–727
- Hibert, M., Trumpp-Kallmeyer, S., Bruinvels, A., and Hoflack, J. (1991) *Mol. Pharmacol.* **40**, 8–15
- Trumpp-Kallmeyer, S., Hoflack, J., Bruinvels, A., and Hibert, M. (1992) *J. Med. Chem.* **35**, 3448–3462
- Almaula, N., Ebersole, B. J., Zhang, D., Weinstein, H., and Sealfon, S. C. (1996) *J. Biol. Chem.* **271**, 14672–14675
- Almaula, N., Ebersole, B. J., Ballesteros, J. A., Weinstein, H., and Sealfon, S. C. (1996) *Mol. Pharmacol.* **50**, 34–42
- Kristiansen, K., and Dahl, S. G. (1996) *Eur. J. Pharmacol.* **306**, 195–210
- Shapiro, D. A., Kristiansen, K., Kroeze, W. K., and Roth, B. L. (2000) *Mol. Pharmacol.* **58**, 877–886
- Lu, Z.-L., Saldanha, J. W., and Hulme, E. C. (2001) *J. Biol. Chem.* **276**, 34098–34104
- Meng, E. C., and Bourne, H. R. (2001) *Trends Pharmacol. Sci.* **22**, 587–593
- Palczewski, K., Kumasaka, T., Hori, T., Behnke, C. A., Motoshima, H., Fox, B. A., Le Trong, I., Teller, D. C., Okada, T., Stenkamp, R. E., Yamamoto, M., and Miyano, M. (2000) *Science* **289**, 739–745
- Teller, D. C., Okada, T., Behnke, C. A., Palczewski, K., and Stenkamp, R. E. (2001) *Biochemistry* **40**, 7761–7772
- Oliveira, L., Paiva, A. C. M., and Vriend, G. (1993) *J. Comput. Aided Mol. Des.* **7**, 649–658
- Baldwin, J. M. (1994) *Curr. Opin. Cell Biol.* **6**, 180–190
- Zhang, D., and Weinstein, H. (1994) *FEBS Lett.* **337**, 207–212
- Ballesteros, J. A., and Weinstein, H. (1995) *Methods Neurosci.* **25**, 366–428
- Roth, B. L., Willins, D. L., Kristiansen, K., and Kroeze, W. K. (1998) *Pharmacol. Ther.* **79**, 231–257
- Thompson, J. D., Plewniak, F., and Poch, O. (1999) *Nucleic Acids Res.* **27**, 2682–2690
- Brooks, B. R., Brucoleri, R. E., Olafson, B. D., States, D. J., Swaminathan, S., and Karplus, M. (1983) *J. Comput. Chem.* **4**, 187–217
- Henderson, R., Baldwin, J. M., Ceska, T. A., Zemlin, F., Beckmann, E., and Downing, K. H. (1990) *J. Mol. Biol.* **213**, 899–929
- Chattopadhyay, A., Rukmini, R., and Mukherjee, S. (1996) *Biophys. J.* **71**, 1952–1960
- Edvardsen, O., Sylte, I., and Dahl, S. G. (1992) *Mol. Brain Res.* **14**, 166–178
- Loric, S., Maroteaux, L., Kellermann, O., and Launay, J.-M. (1995) *Mol. Pharmacol.* **47**, 458–466
- Sealfon, S. C., Chi, L., Ebersole, B. J., Rodic, V., Zhang, D., Ballesteros, J. A., and Weinstein, H. (1995) *J. Biol. Chem.* **270**, 16683–16688
- von Heijne, G. (1991) *J. Mol. Biol.* **218**, 499–503
- Deane, C. M., and Lummis, S. C. R. (2001) *J. Biol. Chem.* **276**, 37962–37966
- Ghinea, G., Padron, G., Hoof, R. W. W., Sander, C., and Vriend, G. (1995) *Proteins Struct. Funct. Genet.* **23**, 415–421
- Hulme, E. C., Lu, Z.-L., Ward, S. D. C., Allman, K., and Curtis, C. A. M. (1999) *Eur. J. Pharmacol.* **375**, 247–260
- Westkaemper, R. B., and Glennon, R. A. (1993) *Med. Chem. Res.* **3**, 317–335
- Donnelly, D., Findlay, J. B., and Blundell, T. L. (1994) *Receptors Channels* **2**, 61–78
- Barak, L. S., Mennard, L., Ferguson, S. S. G., Colapietro, A. M., and Caron, M. G. (1995) *Biochemistry* **34**, 15407–15414
- Wang, C. D., Gallaher, T. K., and Shih, J. C. (1993) *Mol. Pharmacol.* **43**, 931–940
- Choudhary, M. S., Sachs, N., Uluer, A., Glennon, A., Westkaemper, R. B., and Roth, B. L. (1995) *Mol. Pharmacol.* **47**, 450–457
- Roth, B. L., Shoham, M., Choudhary, M. S., and Khan, N. (1997) *Mol. Pharmacol.* **52**, 259–267
- Brouland, J.-P., Manivet, P., Brocheriou-Spelle, I., Wassef, M., Le Bodic, M.-F., Lavergne, A., and Launay, J.-M. (2001) *Endocr. Pathol.* **12**, 77–86
- Schmück, K., Ullmer, C., Kalkman, H. O., Probst, A., and Lübbert, H. (1996) *Eur. J. Neurosci.* **8**, 959–967
- Nebigil, C. G., Hickel, P., Messaddeq, N., Vonesch, J.-L., Douchet, M.-P., Monassier, L., György, K., Matz, R., Andriantsitohaina, R., Manivet, P., Launay, J.-M., and Maroteaux, L. (2001) *Circulation* **103**, 2973–2979